Print ISSN : 0972-8813
e-ISSN : 2582-2780

[Vol. 20(2), May-August, 2022]

Pantnagar Journal of Research

(Formerly International Journal of Basic and Applied Agricultural Research ISSN : 2349-8765)

G.B. Pant University of Agriculture & Technology, Pantnagar

PANTNAGAR JOURNAL OF RESEARCH

Vol. 20(2) May-August, 2022

CONTENTS

Nanosilica induced pathological changes in Wistar rats

NEHA, MUNISH BATRA and R.S. CHAUHAN

Department of Veterinary Pathology, College of Veterinary and Animal Sciences, G.B. Pant University of Agriculture and Technology, Pantnagar-263 145 (U.S. Nagar, Uttarakhand)

ABSTRACT: Thirty-five Wistar rats, six weeks old, of either sex were divided randomly into two groups. Group I comprised of 20 rats as control group and group II having 15 rats as treatment group. Group II was orally administered silicon dioxide (silica) nanoparticles of 20 nm diameter in distilled water at NOAEL dose of 2000mg/kg body weight per day and were gavaged once daily for 90 days. Five rats each were sacrificed at 0 (only from group I), 30th, 60th and 90th DPT and representative tissue samples were collected at these intervals. No lesion could be observed in any organ of any rat of group I at any interval. In group II rats, liver exhibited vascular changes, mononuclear cells infiltration, dilated sinusoidal spaces, Kupffer cells hyperplasia, degeneration and necrosis of hepatocytes. Lungs revealed atelectasis, emphysema, congestion and infiltration of mononuclear cells and thickening of interalveolar septa. Kidneys showed mononuclear cell infiltration in interstitium, alterations in glomeruli, necrosis and sloughing of tubular epithelial cells and obliteration of tubular lumen. Intestine revealed increase in number of goblet cells, necrosis and desquamation of epithelium. Spleen exhibited depletion of lymphoid tissue. Heart showed vascular changes and necrosis of cardiomyocytes. There were vascular changes and mild depletion of lymphoid tissue in thymus. Brain exhibited degeneration and necrosis of neurons and neuronophagia. Ultrastructural studies in liver and kidney revealed accumulation of nanosilica in lysosomes and mitochondria, mitochondrial damage and apoptosis of hepatocytes. It can be concluded from the present studies that nanosilica exerted adverse effects on tissues of Wistar rats at NOAEL dose administered for a period of 90 days.

Key words: Nanosilica, pathology, Wistar rats

Silica nanoparticles in the past decades have drawn considerable scrutiny because of their typical physical attributes, active surface state, exclusive photoluminescence and biocompatibility. Silica nanoparticles are claimed to be present in nearly 100 products out of 846 nano- based products listed in a consumer product inventory (Vance *et al.,* 2015). Synthetic amorphous silica (SAS) is extensively used in processed foods. It is registered by the European Union as a food additive with the code E 551 (E.U. Regulation, 2012), which is also in the nano size range, suggesting that the general population is possibly more exposed than initially expected. SiO_2NPs are utilized for anti-caking and flow improvement in common salt and food powders and also as a thickening or stabilizing agent in emulsions (Merget *et al.,* 2002). A large number of mesoporous silica nanoparticles with largely varied compositions, structures and morphologies have been chemically designed and synthesized, which show very promising application prospects in nano-biomedicine due to their little cytotoxicity, enhanced therapeutic efficiency supports for contrast agents and good biocompatibility (Chen *et al.,* 2013). Due to their enhanced use in various fields, there is need, to study the toxic effects of nanosilica on the body. Silica nanoparticles (SiNPs) are among the priority lists for toxicity assessment by Organization for Economic Co-operation and Development (OECD, 2010). Numerous outcomes of *in vitro* studies have manifested the low cytotoxicities of mesoporous silica nanoparticles against different cell lines (He *et al.,* 2011). Many *in vivo* studies have demonstrated that administration of SiO_2NPs have toxic effects mainly on the liver, spleen, and lung (Xie *et al.,* 2010; Guo *et al.,* 2013). A number of studies have researched the toxicity of SiO_2NPs according to route of exposure. These studies have suggested that there is a variation in the main target organs according to the various routes of administration. Although there have been various studies on the toxicity of nanosilica on various species with various doses and with different roué of administration. There is paucity of studies involving No Observable Adverse Effect Dose (NOAEL). Keeping these facts in mind, the present study was planned to know the toxic effects of nanosilica on the various tissues at NOAEL dose.

MATERIALS AND METHODS

Apparently healthy, six weeks old, 35 Wistar rats of either sex were procured from Laboratory Animal Resources, Indian Veterinary Research Institute, Izatnagar, Bareilly, India. These rats were maintained in Experimental Animal House of Department of Veterinary Pathology, College of Veterinary and Animal Sciences, Pantnagar under standard

managemental conditions. The project was approved by Institutional Animal Ethics Committee, College of Veterinary and Animal Sciences, Pantnagar vide letter number IAEC/CVASc/VPP/327 dated 14-5-2018. All the rats were acclimatized for a period of seven days prior to start of experimentation. Rats were randomly divided in two groups, group I with 20 rats served as control group and provided as lib water and standard ration group II with 15 rats as treatment group. The silicon dioxide (silica) nanoparticles of 20 nm diameter in nanodispersion type A form with molecular weight 60.9 was purchased from Sisco Research Laboratories Pvt. Ltd, India. The nanoparticles were dispersed in distilled water and working samples of recommended dose formulation was prepared daily during the entire period of study. The nanoparticles were homogenized by vortexing just prior to administration and were gavaged once daily for 90 days. The dose used in the study was 2000 mg/kg body weight per day (Kim *et al.,* 2014) which is a No Observable Adverse Effect Level (NOAEL) dose**.** The experimental design in tabular form is given in Table 1:

Table 1: Experimental design in tabulated form

Days post treatment (DPT)	Group I (control)	Group II (treatment)
0 DPT	5 rats	—
30th DPT	5 rats	5 rats
60th DPT	5 rats	5 rats
90th DPT	5 rats	5 rats
Total 35 rats	20 rats	15 rats

Pathological studies

Gross and Histopathological examination

At 0 DPT, five rats from group I, were randomly sacrificed using standard ethical procedures. Thereafter, at 30th, 60th and 90th DPT, five rats each from both the groups were sacrificed using standard ethical procedures. All the rats were subjected to detailed post mortem examination and the gross lesions were duly recorded. For histopathological studies, representative samples were collected in 10% neutral buffered formalin from liver, lung, kidneys, intestines, spleen, heart, thymus and brain. The fixed tissues were processed as per the standard protocol (Luna, 1968).

Transmission electron microscopic studies

Ultra-structural studies of liver, kidney and spleen was done in group II rats at 90th DPT. Representative tissue samples were collected, fixed and sent for further processing to All India Institute of Medical Sciences (AIIMS), Delhi. The representative samples of liver, kidneys and spleen of 1 mm^3 size were fixed in cold glutaraldehyde solution (2.5% v/v in 0.1 M sodium phosphate buffer, pH 7.4) immediately after sacrificing the rats for primary fixation for 24 hours. Secondary fixation of tissues was done with 1% osmium tetra chloride (OsO_4) solution. Dehydration was done in ascending grades of acetone and dry acetone. Clearing of acetone was done with the help of toluene. The tissues were then infiltrated with embedding medium and when the resin gets hardened (polymerized), the tissues were trimmed and sectioned by ultra-microtome. To obtain a good contrast, double staining method using solutions of uranyl acetate and lead citrate were used and observed under the TEM.

RESULTS AND DISCUSSION

Pathomorphological studies

Gross Pathology

There were no observable lesions found during external examination and after opening the carcass in any groups at any interval. No gross lesions could be recorded in any organ of animals of group I rats at any interval. In liver of group II rats, there were presence of pinkish discoloration on the surface of liver at few places at 30th DPT. Lungs of group II rats exhibited only mild congestion and consolidation at 90th DPT. Gross examination of kidneys, intestines, spleen, heart, thymus and brain revealed no observable lesion in group II at any time interval.

Histopathological Examination

Histopathologically, no significant changes were seen in any organ of group I rats throughout the period of study. In group II rats, liver revealed congestion of large blood vessels, infiltration of mononuclear cells, dilatation of sinusoidal spaces, degeneration and necrosis of hepatocytes at few places at 30th DPT. While at 60th DPT, congestion of blood vessel, mononuclear cells infiltration

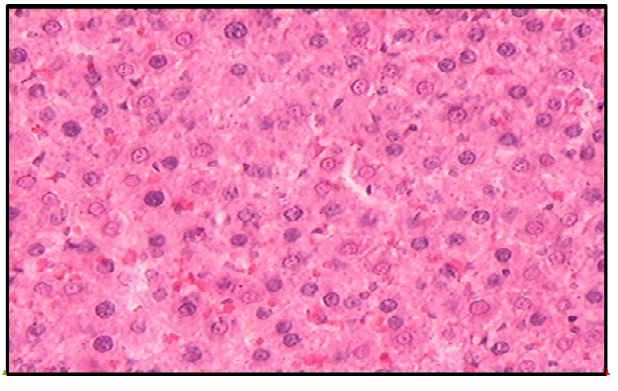

Fig. 1: Photomicrograph of liver depicting degeneration, necrosis of hepatocytes and hyperplasia of Kupffer cells (group II, 90th DPT, H & E X 200)

and necrosis of hepatocytes was evident in liver. At 90th DPT, degeneration and necrosis of hepatocytes at places and proliferation of Kupffer cells was evident (Fig. 1). Lungs of group II rats showed emphysema, thickening of interalveolar septa at 30th DPT (Fig. 2). At 60th and 90th DPT, congestion of blood vessels, atelectasis and emphysema at places and infiltration of mononuclear cells at many places in lung parenchyma was observed in rats of group II rats. Kidneys in group II rats, at 30th DPT, revealed proliferative changes in glomerulus along with loss of Bowman's space. Atrophic glomerulus and necrotic changes in tubular epithelium along with obliteration of lumen of tubules at few places. At 60th DPT, there was necrosis of kidney tubular epithelial cells and obliteration of lumen of tubules at many places in kidneys. At 90th DPT, necrosis and sloughing of tubular epithelial cells was observed in kidneys at few places (Fig. 3). At few places, there was absence of glomerulus from Bowman's capsule, necrosis of kidney tubular epithelial cells and obliteration of tubular lumen at places. Intestine of group II rats showed increase in number of goblet cells, necrosis and desquamation of villous epithelium at 30th DPT (Fig. 4). At 60th and 90th DPT, increased number of goblet cells only was observed. Spleen of group II rats revealed increase in area of red pulp and decrease in area of white pulp at 30th DPT. Depletion of lymphoid cells was observed at 60th and 90th DPT (Fig. 5). Heart evinced mild edema and necrosis of cardiomyocytes in group II rats at 60th DPT (Fig. 6). Congestion in blood vessels and haemorrhages were noticed at 90th DPT in cardiac muscles. Thymus, in group II rats, at 60th DPT, revealed mild depletion of lymphoid tissue. Mild congestion of blood vessel and depletion of lymphoid cells were observed in thymus at 90th DPT. Brain of group II rats depicted degeneration and necrosis of neurons, satellitosis and neuronophagia at 90th DPT only (Fig. 7).

Ultrastructural study of liver

Transmission electron microscopy (TEM) of liver of group II rats at 90th DPT revealed apoptosis of hepatocytes showing chromatin condensation and segregation of nucleus into apoptotic bodies along with condensation of cytoplasm (Fig. 8), Kupffer cells lying in sinusoidal spaces and accumulation of nanosilica particles in the lysosomes

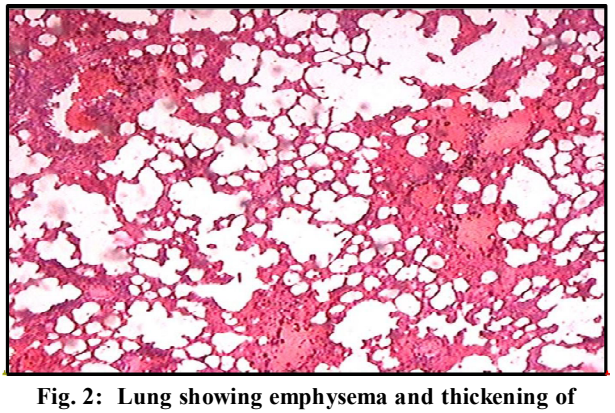

Fig. 2: Lung showing emphysema and thickening of interalveolar septa (group II, 30th DPT, H& E X 40)

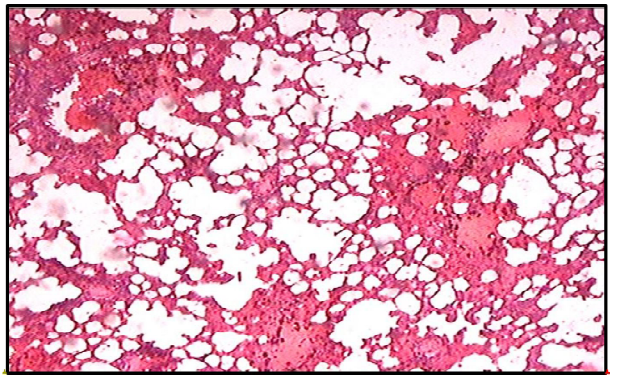

Fig. 3: Photomicrograph of kidney depicting segmentation of glomerulus, necrosis and sloughing of kidney tubular epithelial cells (group II, 90th DPT, H & E X 100)

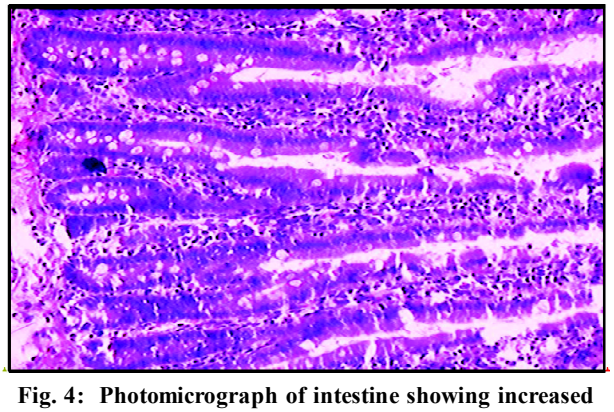

Fig. 4: Photomicrograph of intestine showing increased number of goblet cell, and necrosis and desquamation of villous epithelium (group II rat, 30th DPT H & E X 100)

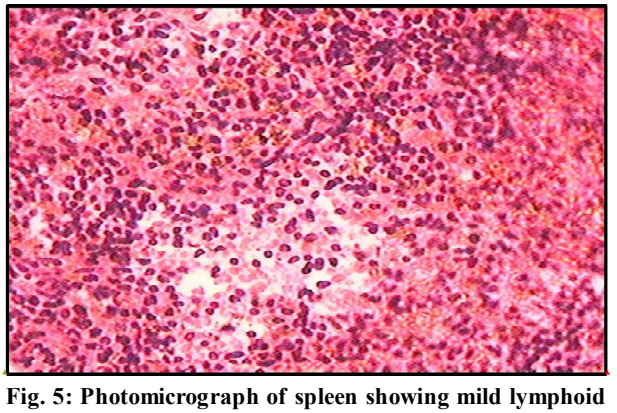

Fig. 5: Photomicrograph of spleen showing mild lymphoid depletion (group II, 60th DPT, H & E X 100)

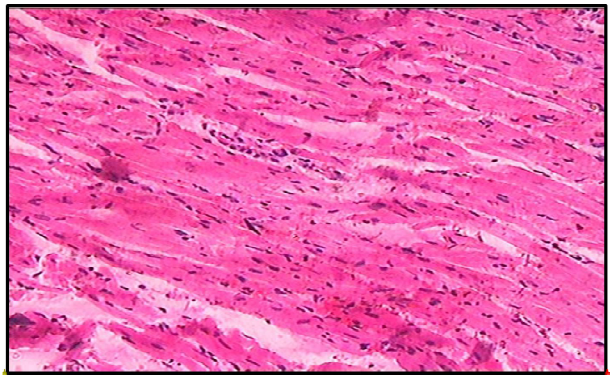

Fig. 6: Photomicrograph of heart showing, mild edema and necrosis of cardiac muscle cells (group II, 60th DPT (H & E X100)

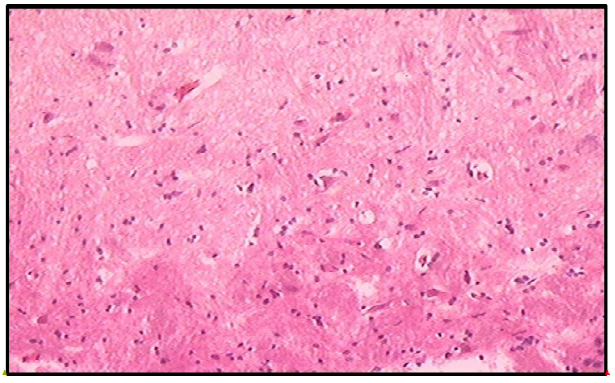

Fig. 7: Photomicrograph of brain showing degeneration and necrosis of neurons, satellitosis and neuronophagia (group II, 90th DPT, H & E X 100)

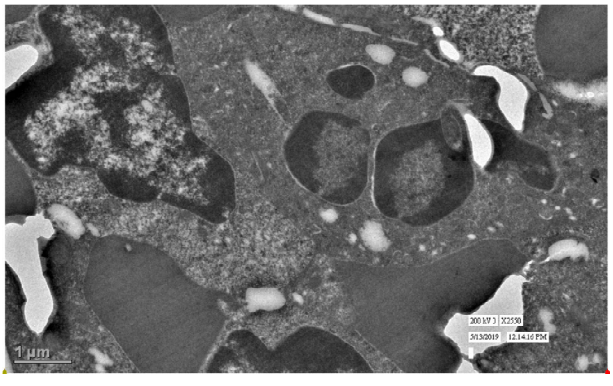

Fig. 8: Transmission electron micrograph of hepatocytes undergoing apoptosis with chromatin condensation and segregation of nucleus into apoptotic bodies along with condensation of cell cytoplasm (group II X 2550)

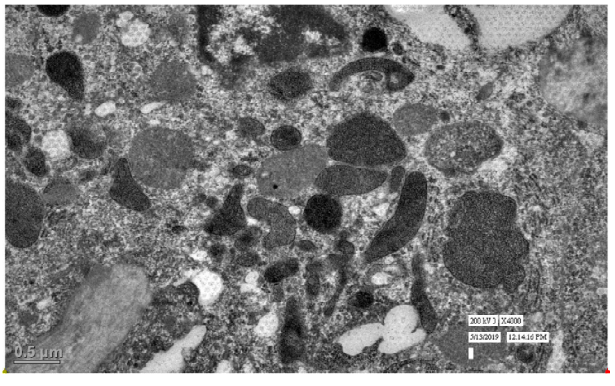

Fig. 9: Transmission electron micrograph of lysosome containing nanosilica in particulate form in liver (group II X 4000)

(Fig. 9). Ultrastructural studies of kidneys at 90th DPT in group II rats, revealed accumulation of electron dense bodies suggesting silica nanoparticles in form of aggregates in lysosomes and in mitochondria (Fig. 10) along with swelling of mitochondria and loss of cristae (Fig. 11).

In the present study, grossly, there were no significant changes in organs of group I rats throughout the period of study. Liver of few rats in group II revealed pinkish discoloration over the surface. Lungs revealed congestion and consolidation. No records regarding any adverse effects of nanosilica on gross pathology of rats at the NOAEL dose (2000mg/kg BW) has been documented till now as per the literature available. The present study also suggests that nanosilica at this dose rate do not cause any apparent gross change in various organs of the body.

There were no significant histopathological changes in liver of the group I rats throughout the period of study. In group II rats, liver exhibited congestion of blood vessels, mononuclear cells infiltration, dilatation of sinusoidal spaces, hydropic degeneration, coagulative necrosis of hepatocytes and proliferation of Kupffer cells (KC). Similar lesions have been described by Liu *et al.,* (2011) and Hassankhani *et al.* (2014) in liver of silica nanoparticle treated mice. Parveen *et al.* (2012) reported degenerative changes in hepatocytes in Wistar rats after sub-chronic intra- nasal exposure. Kupffer cell (KC) proliferation, oxidative stress and hepatic inflammation were observed in liver of rats by Chen *et al.* (2013). By these findings it is evident that nanosilica induces inflammation in the liver. The number of KCs in sinusoids was found to be increased after administration of silica NPs, which indi-cated that silica NPs has a role in activation of the phagocytic activity of KCs by elevating the their number to remove depositing nanoparticles (Abdelhalim and Jarrar, 2011). Kupffer cells are the principal responders to a toxicant and the molecules released after their interaction with toxicants are regarded mediators of succeeding hepatic damage (Laskin and Laskin, 2001). *In vitro* exposure to silica NPs stimulated KCs to release reactive oxygen species, tumour necrosis

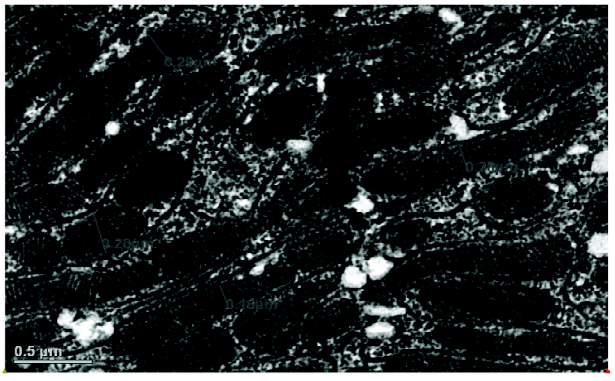

Fig. 10: Transmission electron micrograph of kidney showing deposition of nanosilica particles in mitochondria and swollen mitochondria at places along with loss of cristae (group II X 4000)

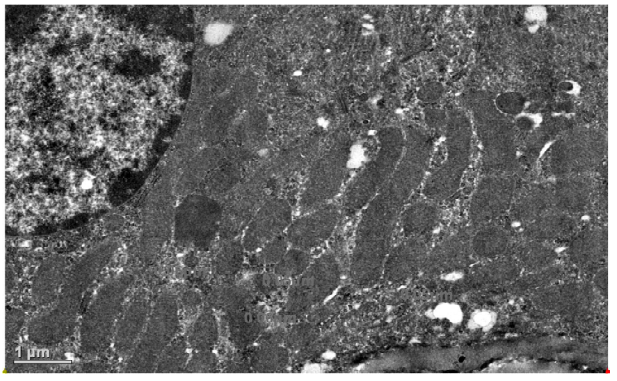

Fig. 11: Transmission electron micrograph of kidney showing swelling of mitochondria with loss of cristae (group II X 2550)

factor –α and nitric oxide in large amounts (Chen *et al.,* 2013). These released substances are responsible for further damage to the hepatic tissue. In lungs, emphysema, atelectasis at places, congestion and infiltration of mononuclear cells leading to thickening of interalveolar septa was observed at all DPT with increasing severity from 0 to 90th DPT. These results were in confirmation with Hassankhani *et al*. (2014) who administered nanosilica to mice at dose of 333 mg/kg BW. Yang *et al.* (2013) reported congestion in lungs and thickened interstitium in nanosilica treated mice. Kaewamatawong *et al.* (2006) reported pulmonary inflammation after intra-tracheal instillation of nanosilica in mice. Thickening of interalveolar septa due to infiltration of mononuclear cells leads to atelectasis of alveoli. Further the alveoli in adjacent areas fuse to accumulate more air in compensation to atelectasis leading to emphysema. The generation of reactive oxygen species (ROS) by nanosilica particles and cells of immune system activated by them lead to inflammation, lung tissue damage. The persistence of these transformed cells in silicosis is thought to be due to release of proinflammatory cytokines during inflammation **(**Huaux, 2007). Kidney of group II rats revealed haemorrhages and infiltration of mononuclear cells in interstitial tissues, proliferative changes in glomerulus along with loss of space between glomerulus and basement membrane, segmentation of glomerulus, atrophic glomerulus, complete loss of glomerulus at few places, necrotic changes in tubular epithelium along with sloughing of kidney tubular cells and obliteration of lumen of tubules. These results are in confirmation with Hassankhani *et al*. (2014) in silica nanoparticles administered mice. He *et al*. (2011), also reported accumulation of these nanoparticles in kidneys and damage caused by them. The pathological examinations revealed that silica nanoparticles have serious toxicological effects on renal tissue (Kim *et al.,* 2014). Silica NPs could induce kidney injury via the activation of NF-kB signaling pathways (Chen *et al.,* 2015). Intestine of group II rats revealed increased number of goblet cells and necrosis and sloughing of villous epithelium. Intestine is the first organ which comes in contact with these nanoparticles after oral administration. These nanoparticles may act as mild irritants to the intestinal mucosa which can be confirmed by presence of increased number of goblet cells. Spleen of group II rats revealed hyperplasia of red pulp, mild depletion of lymphoid tissue and hemosiderosis. Lee *et al.* (2014) observed that different organs such as spleen, liver, lungs and kidneys were principal target of colloidal silicaNPs with varied sizes administered to rats via gavaging. Zande *et al.* (2014), Li *et al.* (2013) and Yu *et al.* (2012) revealed spleen and liver as main target organ in nanosilica toxicity after gavaging, intravenous and intraperitoneal administration, respectively. A decrease in white pulp in spleen was observed by Lee *et al.* (2013). Spleen is considered as an important organ for initiation of immune responses. Spleen is found to be highly sensitive to harmful effects of xenobiotics. In group II, heart revealed congestion in blood vessels, haemorrhages, fragmentation of cardiac muscles, edema and necrosis of cardiomyocytes. Alterations in the myocardium including capillary congestion and interstitial edema were also noted by Zhuravskii *et al.* (2016). Thymus revealed congestion, haemorrhage, mild depletion of lymphoid tissue. Studies on effect of these particles on thymus are rare and not documented in literature available. In brain tissues degeneration and necrosis of neurons, satellitosis and neuronophagia was observed in group II rats. The long-term adverse effects of deposition of nanoparticles in the brain have also been reported by Wu *et al.* (2011). Kleinman *et al.*

(2008), have also reported that nanosilica enters the brain after crossing blood brain barrier when deposited in nasal olfactory area and causes injury to CNS. Very low levels of SiNPs can alter microglial function (Choi *et al.,* 2010). The possible mechanism for cell dysfunction and cytotoxicity may be the release of proinflammatory mediators from the microglial cells after being activated by nanosilica particles (Xue *et al.,* 2012).

In ultrastructural studies, liver of group II rats revealed apoptosis in hepatocytes with characteristic chromatin condensation, rearrangement and formation of apoptotic bodies along with condensed cytoplasm, KCs with vacuole lying in sinusoidal spaces, presence of silica nanoparticles in lysosomes. Oxidative stress induced by NPs could damage the cellular components and lead to cell death via apoptosis (Fu *et al.,* 2014). Silica NPs in hepatocytes both within membrane-bound vesicles and, as intracytoplasmic inclusions were detected by Xue *et al.* (2014). Small NPs of diameter 10–40nm can pass through lipid bilayers by passive mechanism (Sun *et al.,* 2011). Silica nanoparticles of size 40–80 nm can gain access to the cell nucleus and concentrate to distinct domains around the nucleoplasm, while coarse particles get completely deposited in the cell cytoplasm (Hirai *et al.,* 2012). Nanosilica can induce apoptosis via the releasing cytochrome C enzymes from mitochondria and further activation of caspase 3 enzyme. Moreover, changes in the expression of apoptosis associated proteins in the mitochon-drial signaling pathway could be a reason for apoptosis (Yang *et al.,* 2019). Kidney revealed deposition of nanosilica aggregates in lysosomes, mitochondria along with swelling of mitochondria and loss of cristae. The presence of silica nanoparticles in lysosomes and endocytic compartments was confirmed by Tarantini *et al.* (2015) by electron microscopy. Particulate forms of silica were found in the liver and kidneys which was confirmed by transmission electron microscopy analysis. Transmission electron microscopy and energy dispersive spectroscopy analysis in tissues revealed almost intact particles in liver, but partly decom-posed particles with non- uniform shape and size were noted in kidneys, particularly in rats that had been administered 20 nm nanoparticles (Lee *et al.,* 2014).
Collectively our results suggest that nanosilica have toxic effects on tissues even at NOAEL dose on the repeated exposure.

CONCLUSION

It can be concluded from the present study that nanosilica have adverse effects on various tissues leading to hepatopathy, nephropathy and immunopathy in particular in Wistar rats at NOAEL dose for a period of 90 days.

ACKNOWLEDGEMENTS

The authors are thankful to Dean, College of Veterinary and Animal Sciences, GB Pant University of Agriculture and Technology, Pantnagar for providing financial help to carry out this research work.

REFERENCES

Abdelhalim, M.A. and Jarrar, B.M. (2011). Gold nanoparticles administration induced prominent inflammatory, central vein intima disruption, fatty change and Kupffer cells hyperplasia. *Lipids Health Dis*., 10:133.

Chen, Q., Xue, Y. and Sun, J. (2013). Kupffer cell-mediated hepatic injury induced by silica nanoparticles in vitro and in vivo. *International Journal of Nanomedicine,* 8: 1129- 1140.

Chen, X., Zhouhua, W., Jie, Z., Xinlu, F., Jinqiang, L., Yuwen, Q. and Zhiying, H. (2015). Renal interstitial fibrosis induced by high-dose mesoporous silica nanoparticles via the NF-kappaB signaling pathway. *International Journal of Nanomedicine,* 10:1–22.

Choi, J., Zheng, Q., Katz, H. E. and Guilarte, T. R. (2010). Silica based nanoparticle uptake and cellular response by primary microglia. *Environmental Health Perspectives*, 118: 589–595.

European Union Commission Regulation (EU) No 231/ 2012 of 9 March 2012 laying down specifications for food additives listed in Annexes II and III to Regulation (EC) No 1333/2008 of the European Parliament and of the Council. *Off J Eur Union.,* 2012; 2012(83): 1–29.

Fu, P.P., Xia, Q., Hwang, H.M., Ray, P.C. and Yu, H. (2014). Mechanisms of nanotoxicity: generation of reactive oxygen species. *Journal of Food and Drug Analysis*., 22 (1): 64- 75.

Guo, M., Xu, X., Yan, X., Wang, S., Gao, S. and Zhu, S. (2013). In vivo biodistribution and synergistic toxicity of silica nanoparticles and cadmium chloride in mice. *Journal of Hazardous Materials,* 260:780–788.

Hassankhani, R., Esmaeillou, M., Tehrani, A.A., Nasirzadeh, K., Khadir, F. and Maadi, H. (2014). *In vivo* toxicity of orally administrated silicon dioxide nanoparticles in healthy adult mice. *Environmental Science and Pollution Research*, 22(2): 1127-1132.

He, Q., Zhang, Z., Gao, F., Li, Y. and Shi, J. (2011). *In*

vivo biodistribution and urinary excretion of mesoporous silica nanoparticles: effects of particle size and PEGylation. *Small*, 7: 271–280.

Hirai, T., Yoshioka, Y., Takahashi, H., Ichihashi, K.I., Yoshida, T., Tochigi, S., Nagano, K., Abe, Y., Kamada, H., Tsunoda, S.I. and Nabeshi, H. 2012. Amorphous silica nanoparticles enhance cross-presentation in murine dendritic cells. *Biochemical and Biophysical Research Communications*, 427(3): 553-556.

Huaux, F. (2007). New developments in the understanding of immunology in silicosis. *Current Opinion in Allergy and Clinical Immunology*, 7(2): 168-173.

Kaewamatawong, T., Shimada, A., Okajima, M., Inoue, K. and Takano, H. (2006). Acute and subacute pulmonary toxicity of low dose of ultrafine colloidal silica particles in mice after intratracheal instillation. *Toxicologic Pathology*, 34 (7): 958–965.

Kim, Y.R., Lee, S.Y., Lee, E.J., Park, S.H., Seong, N.W., Seo, H.S., Shin, S.S., Kim, S.J., Meang, E.H., Park, M.K. and Kim, M.S. (2014). Toxicity of colloidal silica nanoparticles administered orally for 90 days in rats. *International Journal of Nanomedicine,* 9(2): 67.

Kleinman, M.T., Araujo, J.A., Nel, A., Sioutas, C., Campbell, A., Cong, P.Q., Li, H. and Bondy, S.C. (2008). Inhaled ultrafine particulate matter affects CNS inflammatory processes and may act via MAP kinase signaling pathways. *Toxicology Letters*, 178(2): 127-130.

Laskin, D.L. and Laskin, J.D. (2001). Role of macrophages and inflammatory media-tors in chemically induced toxicity. *Toxicology,* 160: 111–118.

Lee, J.A., Kim, M.K., Paek, H.J., Kim, Y.R., Kim, M.K., Lee, J.K., Jeong, J. and Choi, S.J. (2014). Tissue distribution and excretion kinetics of orally administered silica nanoparticles in rats. *International Journal of Nanomedicine*, 9: 251-260.

Lee, S., Kim, M.S., Lee, D., Kwon, T.K., Khang, D., Yun, H.S. and Kim, S.H. (2013). The comparative immunotoxicity of mesoporous silica nanoparticles and colloidal silica nanoparticles in mice. *International Journal of Nanomedicine*, 8: 147.

Li, X., Chen, Y., Wang, M., Ma, Y., Xia, W. and Gu, H. (2013). A mesoporous silica nanoparticle–PEI–fusogenic peptide system for siRNA delivery in cancer therapy. *Biomaterials*, 34(4): 1391-1401.

Liu, T., Li, L., Teng, X., Huang, X., Liu, H., Chen, D., Ren, J., He, J. and Tang, F. (2011). Single and repeated dose toxicity of mesoporous hollow silica nanoparticles in intravenously exposed mice. *Biomaterials*. 32(6): 1657-1668.

Luna, L. G. (1968). Manual of histologic staining methods of the Armed Forces Institute of Pathology.

Merget, R., Bauer, T., Kupper, H.U., Philippou, S., Bauer, H.D., Breitstadt, R. and Bruening, T. (2002). Health hazards due to the inhalation of amorphous silica. *Archives of Toxicology,* 75: 625- 634.

OECD (2010). O. F. E. C.-O. A. D. Series on the safety of manufactured nanomaterials No. 27-ENV/JM/MONO (2010)46. Available at: http://www.oecd.org/science/ nanosafety/. assessed on 25th December 2018.

Parveen, A., Rizvi, S.H.M., Gupta, A., Singh, R., Ahmad, I., Mahdi, F. and Mahdi, A.A. (2012). NMR-based metabonomics study of sub-acute hepatotoxicity induced by silica nanoparticles in rats after intranasal exposure. *Cell. Mol. Biol.*, 58(1): 196-203.

Sun, L., Li, Y., Liu, X., Jin, M., Zhang, L., Du, Z., Guo, C., Huang, P. and Sun, Z. (2011). Cytotoxicity and mitochondrial damage caused by silica nanoparticles. *Toxicology in vitro*, 25(8): 1619-1629.

Tarantini, A., Lanceleur, R., Mourot, A., Lavault, M.T., Casterou, G., Jarry, G., Hogeveen, K. and Fessard, V. (2015). Toxicity, genotoxicity and proinflammatory effects of amorphous nanosilica in the human intestinal Caco-2 cell line. *Toxicology in vitro*, 29(2): 398-407.

Vance, M.E., Kuiken, T., Vejerano, E.P., McGinnis, S.P., Hochella Jr, M.F., Rejeski, D. and Hull, M.S. (2015). Nanotechnology in the real world: redeveloping the nanomaterial consumer products inventory. *Beilstein Journal of Nanotechnology,* 6: 1769–1780.

Wu, J., Wang, C., Sun, J. and Xue, Y. (2011). Neurotoxicity of silica nanoparticles: brain localization and dopaminergic neurons damage pathways. *ACS nano*, 5(6): 4476-4489.

Xie, G., Sun, J., Zhong, G., Shi, L. and Zhang, D. (2010). Biodistribution and toxicity of intravenously administered silica nanoparticles in mice. *Archives of Toxicology*, 84(3): 183-190.

Xue, Y., Chen, Q., Ding, T. and Sun, J. (2014). SiO_2 nanoparticle-induced impairment of mitochondrial energy metabolism in hepatocytes directly and through a Kupffer cell-mediated pathway *in vitro*. *International Journal of Nanomedicine*, 9: 2891.

Xue, Y., Wu, J. and Sun, J. (2012). Four types of inorganic nanoparticles stimulate the inflammatory reaction in brain microglia and damage neurons *in vitro*. *Toxicology Letter,* 214(2): 91–98.

Yang, Y., Du, X., Wang, Q., Liu, J., Zhang, E., Sai, L., Peng, C., Lavin, M.F., Yeo, A.J., Yang, X. and Shao, H. (2019). Mechanism of cell death induced by silica nanoparticles in hepatocyte cells is by apoptosis. *International Journal of Molecular Medicine*. DOI:10.3892/ijmm.2019.4265

Yang, Y.X., Song, Z.M., Cheng, B., Xiang, K., Chen, X.X., Liu, J.H. and Wang, H. (2013). Evaluation of the toxicity of food additive silica nanoparticles on gastrointestinal cells. *Journal of Applied Toxicology*, 34(4): 424–435.

Yu, T., Hubbard, D., Ray, A. and Ghandehari, H. (2012). In vivo biodistribution and pharmacokinetics of silica nanoparticles as a function of geometry, porosity and surface characteristics. *Journal of Controlled Release*, 163(1): 46-54.

Zande, M., Vandebriel, R.J., Groot, M.J., Kramer, E., Rivera, Z.E., Rasmussen, K., Ossenkoppele, J.S., Tromp, P., Gremmer, E.R., Peters, R.J., Hendriksen, P.J., Marvin, H.J., Peijnenburg, A.A. and Bouwmeester, H. (2014). Sub-chronic toxicity study in rats orally exposed to nanostructured silica. *Particle and Fibre Toxicology*, 11: 8.

Zhuravskii, S., Yukina, G., Kulikova, O., Panevin, A., Tomson, V., Korolev, D. and Galagudza, M. (2016). Mast cell accumulation precedes tissue fibrosis induced by intravenously administered amorphous silica nanoparticles. *Toxicology Mechanisms and Methods*, 26(4): 260-269.

Received: August 20, 2022
Accepted: August 29, 2022